Biogeosciences Discuss., 12, 981–1013, 2015
www.biogeosciences-discuss.net/12/981/2015/
doi:10.5194/bgd-12-981-2015

Biogeosciences Discussions
Open Access

Primary productivity and its correlation with rainfall on Aldabra Atoll

J. Shekeine[1], **L. A. Turnbull**[2], **P. Cherubini**[3], **R. de Jong**[4], **R. Baxter**[1], **D. Hansen**[1], **N. Bunbury**[5], **F. Fleischer-Dogley**[5], and **G. Schaepman-Strub**[1]

[1]Institute of Evolutionary Biology and Environmental Studies, University of Zurich, Zurich, 8057, Switzerland
[2]Department of Plant Sciences, University of Oxford, Oxford OX1 3RB, UK
[3]Swiss Federal Institute for Forest, Snow and Landscape Research WSL, 8903 Birmensdorf, Switzerland
[4]Remote Sensing Laboratories, Department of Geography, University of Zurich, Zurich, 8057, Switzerland
[5]Seychelles Islands Foundation, P.O. Box 853, Victoria, Mahe, Seychelles

Received: 22 October 2014 – Accepted: 10 December 2014 – Published: 16 January 2015

Correspondence to: J. Shekeine (shekeinespere@gmail.com)

Published by Copernicus Publications on behalf of the European Geosciences Union.

Abstract

Aldabra Atoll, a UNESCO World Heritage Site since 1982, hosts the world's largest population of giant tortoises. In view of recent rainfall declines in the East African region, it is important to assess the implications of local rainfall trends on the atoll's ecosystem and evaluate potential threats to the food resources of the giant tortoises. However, building an accurate picture of the effects of climate change requires detailed context-specific case-studies, an approach often hindered by data deficiencies in remote areas. Here, we present and analyse a new historical rainfall record of Aldabra atoll together with two potential measures of primary productivity: (1) tree-ring measurements of the deciduous tree species *Ochna ciliata* and, (2) satellite-derived NDVI (normalized difference vegetation index) data for the period 2001–2012. Rainfall declined by about 6 mm yr^{-1} in the last four decades, in agreement with general regional declines, and this decline could mostly be attributed to changes in wet-season rainfall. We were unable to cross-date samples of *O. ciliata* with sufficient precision to deduce long-term patterns of productivity. However, satellite data were used to derive Aldabra's land surface phenology (LSP) for the period 2001–2012 which was then linked to rainfall seasonality. This relationship was strongest in the eastern parts of the atoll (with a time-lag of about six weeks between rainfall changes and LSP responses), an area dominated by deciduous grasses that supports high densities of tortoises. While the seasonality in productivity, as reflected in the satellite record, is correlated with rainfall, we did not find any change in mean rainfall or productivity for the shorter period 2001–2012. The sensitivity of Aldabra's vegetation to rainfall highlights the potential impact of increasing water stress in East Africa on the region's endemic ecosystems.

BGD

12, 981–1013, 2015

1 Introduction

Terrestrial ecosystems of semi-arid oceanic islands are some of the most vulnerable to the effects of climate change (Mimura et al., 2007). Extreme geographical isolation has protected these ecosystems from human interference for the larger part of history. However, in the event of lasting changes in the islands' microclimates, such isolation severely limits the resilience of their endemic inhabitants and ecosystems (Whittaker and Fernández-Palacios, 2007). Climate change on Aldabra Atoll in the Indian Ocean therefore has the potential to severely threaten local biodiversity, as it hosts many floral and faunal endemics together with the world's largest population of giant tortoises. The tortoises dominate the atoll's terrestrial food chain (Gibson and Phillipson, 1983a), grazing primarily on a community of grasses, sedges and herbs that are collectively referred to as "tortoise turf" (Merton et al., 1976). Aldabra was designated as a UNESCO World Heritage Site in 1982 and continues to exhibit ecological phenomena long extinct in similar subtropical islands, e.g., domination of its terrestrial food chain by a reptilian herbivore (Hansen et al., 2010). A recent assessment by the International Union for Conservation of Nature (IUCN) identified climate change as a potentially high threat and the urgent need to initiate research to investigate the potential impact of climate change on the atoll's biodiversity. This includes climate-driven changes in vegetation ecology that can cascade up through the ecosystem and affect plant-animal interactions (Osipova et al., 2014).

Since 1950 there has been an increase in water stress in most parts of sub-tropical Africa (Dai et al., 2004; Mu et al., 2013), characterized mainly by a drop in wet season rainfall (Lyon and DeWitt, 2012). These declines in rainfall have been accompanied by declines in gross primary productivity (GPP) in various locations (Zhao and Running, 2010; Potter et al., 2012). These GPP declines are expected to continue in the future as the frequency and severity of droughts intensifies (Easterling, 2000). Aldabra's wet season occurs during the north-west monsoon (November–April) (Stoddart and Mole, 1977) and the dry season during the south-east monsoon (May–October). Mean intra-

BGD
12, 981–1013, 2015

annual temperature is between 24 and 28 °C (Appendix B, Fig. B1), making rainfall the most likely factor limiting GPP. Given the close coupling between rainfall and the productivity of the tortoise turf (Gibson and Phillipson, 1983a), declines in rainfall are inevitably of concern, as this vegetation type hosts the highest densities of tortoises (Turnbull et al., 2015). Forecasted declines in wet season rainfall over eastern Africa could impact Aldabra's GPP strongly enough to jeopardize its tortoise population and other indigenous biodiversity in the future. In this study, we examine whether Aldabra's rainfall is declining, and whether there are detectable impacts on the atoll's GPP.

Several studies have used the normalized difference vegetation index (NDVI), derived from optical satellite sensors to infer land surface phenology (LSP) and its relationship with rainfall fluctuations in Africa (e.g. Eklundh, 2003; Omuto et al., 2010). In some of these ecosystems, dramatic fluctuations in rainfall induce not only seasonal oscillations in NDVI, but also the formation of annual growth rings in the cambia of some tree species (Fichtler et al., 2004). We combine meteorological data, deciduous tree-ring analysis, and NDVI to analyze long-term trends and intra-annual variability of rainfall and productivity proxies. More specifically, we aim to:

1. Investigate long-term trends in Aldabra's instrumental rainfall record.
2. Assess the dendroecological potential of the indigenous tree, *Ochna ciliata* and – if possible – use these measurements to assess long-term changes in Aldabra's mean primary productivity.
3. Investigate the relationship between land surface phenology and rainfall over the short term (2001–2012).

BGD
12, 981–1013, 2015

2 Materials and methods

2.1 Study site description

Aldabra is a raised coral atoll that lies about 1100 km north-west of Mahé, the principal island of the Seychelles (9°25′0.05″ S 46°24′59.94″ E). The atoll rises to a maximum altitude of 8 m a.s.l. and is comprised of four main islands: Grande Terre, Malabar, Picard and Polymnie (Fig. 1). All islands with the exception of Polymnie host extant populations of giant tortoises.

Aldabra's landscape comprises mainly of shrubs of varying height, either in continuous extents or in a mosaic with open rocky ground carrying a variable cover of grasses and sedges (Hnatiuk and Merton, 1979). Eastern Grande Terre (GTE) is characterized by several types of "mixed scrub" vegetation, which comprises low density shrub, woody types and a ground layer vegetation of tortoise turf grasses (Gibson and Phillipson, 1983b). The rest of the atoll is dominated by the evergreen *Pemphis acidula* (hereafter "Pemphis") shrub that occurs in association with grasses, herbs and other shrub types (Hnatiuk and Merton, 1979).

2.2 Rainfall data record and processing

Monthly rainfall data (based on rain gauge readings) were recorded consistently at the research station on Picard since 1969 (Appendix B): first by the Royal Society of London, and from 1981 onwards, by the Seychelles Islands Foundation. The last four decades in this dataset have complete monthly entries, although there are gaps in the earlier records. A typical "rainfall year" on Aldabra begins with the wet season which runs from November to April and is followed by a dry season which typically runs to the end of October. These seasons are driven by the north-west (wet season) and south-east (dry season) monsoon winds (Farrow, 1971; Stoddart and Mole, 1977). The monthly rainfall data were therefore aggregated over the respective November–October periods (e.g., annual rainfall for year 2000 is the sum of rainfall from

November 1999 to October 2000). The resulting annual series was then regressed against year using ordinary least squares regression for the period 1969–2012, excluding years 1992 and 1993 (no data) and 1976 (missing October rainfall).

Daily rainfall records have been maintained since the year 2000, coinciding with the operational period of the Moderate Resolution Imaging Spectroradiometer (MODIS) sensors aboard NASA's Terra satellite. The daily rainfall data from 2000–2013 were averaged into a 16 day series to match the temporal resolution of the MODIS NDVI data for subsequent rainfall–NDVI analyses. Rainfall seasonality metrics were derived as described in Sect. 2.4.

2.3 Dendrochronological data and processing

Forty-five *Ochna ciliata* (hereafter *O. ciliata*) trees were sampled at Picard, GTE and GTSC (Grande Terre South-Central) sites in October 2012 (Fig. 1). One radial cross-section was sampled from each tree at breast height. In the laboratory, 32 cross-sections selected for the dendroecological analysis were sanded with progressively finer abrasive paper to reveal the growth zones and ring boundaries. Digital images of the sanded cross-sections were obtained at 1200 dpi using an Epson 10000XL flatbed scanner. Micro-sections of about 15 µm thickness were then sliced from the cross-sections using a sliding microtome after which they were stained with safranin-astra blue solution, dehydrated through an ethanol series (70, 95, 100 %) and clarified in xylol (Rossi et al., 2013). Fixed slides were then prepared by embalming the stained micro-sections in Canada balsam and drying them for 24 h at 60 °C. Digital images of these slides were then acquired at ×20 magnification using a light microscope (Olympus Bx41 microscope, Japan) equipped with a camera (Canon EOS 650D).

Tree-ring chronologies were developed using standard dendrochronological procedures (Stokes and Smiley, 1968). Tree-rings were identified from the micro-section images and their widths measured from pith to bark using WinDendro software Version 2008a (Regent Instruments Inc., 2008). Resulting chronologies were then cross-dated visually by checking anomalies such as false or missing rings observed

BGD
12, 981–1013, 2015

on the micro-sections against digital scans of the respective tree cross-section. We used the percentage of sign agreement in interannual ring width variation to statistically evaluate the degree of congruence amongst chronologies within and across samples (Schweingruber, 1988).

2.4 NDVI data record and processing

The NDVI data product used to derive LSP metrics was obtained from the MODIS sensor aboard the Terra satellite. The product, Collection 5 VI MOD13Q1, was downloaded for the period 2000–2012 (Oak Ridge National Laboratory Distributed Active Archive Center (ORNL DAAC), 2011). The product has a spatial resolution of 250 m and a temporal resolution of 16 days. NDVI is computed as a normalized ratio of the reflectances in the near infra-red (NIR) and red spectral ranges:

$$\mathrm{NDVI} = \frac{\rho_{\mathrm{NIR}} - \rho_{\mathrm{RED}}}{\rho_{\mathrm{NIR}} + \rho_{\mathrm{RED}}} \quad (1)$$

Where ρ is the reflectance integrated between 0.841 and 0.876 µm (NIR, MODIS Band 2) and between 0.62 and 0.67 µm (RED, MODIS Band 1) respectively (Huete et al., 2002).

The product is delivered with the following pre-processing. To minimize the negative bias clouds exert on NDVI, the maximum NDVI value from ca. 10 observations made in each 16 day window is retained to represent that period (Holben, 1986). The MOD13Q1 product is computed from MODIS surface reflectances that have been masked for water, clouds, aerosols, and cloud shadows (Huete et al., 2002). While the product is not corrected for reflectance anisotropy, it comes at the highest spatial resolution (250 m) that MODIS offers; an important advantage when working with spatial extents that are as small and heterogeneous as Aldabra. Quality filtering during pre-processing is done on a per-pixel basis (Huete et al., 2002). Some pixels close to the ocean were inconsistently classified as water or land areas by the MODIS land/water mask.

Therefore, we excluded pixels that had NDVI values of less than 0 (indicating water) for more than half of the studied period.

The distribution of vegetation types on Aldabra were mapped based on a vegetation survey conducted in 1983 (Fig. 1). Key vegetation types were (a) mixed scrub of varying shrub density (on GTE) and (b) Pemphis shrub that dominates the rest of Aldabra's terrestrial zone. This distinction correlates strongly with spatial patterns in the atoll's geomorphology and physiography (Trudgill, 1979). From field observations, these vegetation and physiographic patterns have persisted to date. There is no current research on spatial distribution of vegetation types on the atoll beyond this level of generalization. We therefore stratified our analyses by six sites based on the map by Gibson, 1983 (Fig. 1). NDVI values from all pixels within a site were spatially averaged for each 16 day period 2000–2012, yielding six site chronologies (Table 1).

Derivation of LSP metrics typically involves fitting smoothing functions to raw NDVI time series and estimating the desired metrics from the smoothed data (Garonna et al., 2014). We used smoothing algorithms implemented in the TIMESAT software (Jönsson and Eklundh, 2004). Phenological parameters were extracted for the NDVI time series at each site. Goodness of fit was assessed using the root mean square error (RMSE, Table 1), as well as qualitatively by visual examination of the accuracy of start of season (SOS) and end of season (EOS) detection. Based on these two criteria, the Savitzky–Golay filter applied with an STL (Seasonal decomposition of Time series by Loess) outlier handler gave the best result.

Fluctuations in NDVI time series that are not related to changes in vegetation states, i.e., noise, are a common problem in LSP. The problem is partly due to cloud effects that are not resolved by the cloud mask during the pre-processing of the vegetation index and can impede accurate detection of phenological parameters (Jönsson and Eklundh, 2004). RMSE reduced with the increase in the spatial extent of the study sites (Table 1), possibly because larger areas tended to have more cloud free pixels. For each site series, these noise effects were minimized by iterating the Savitzky–Golay smoother upward several times so as to adapt it to the upper envelope of the NDVI time

BGD
12, 981–1013, 2015

series (Jönsson and Eklundh, 2004). Finally, LSP parameters were extracted for each site's NDVI time series for the 12 growing seasons spanning the period 2001–2012 as follows:

i. Start of season (SOS): day of year at which 10 % of the NDVI range between previous dry season minimum and current growing season maximum is reached.

ii. End of season (EOS): day of year at which 10 % of the NDVI range between the current growing season maximum and next dry season minimum is reached.

iii. Length of season (LOS): arithmetic difference (in days) between SOS and EOS.

Value based seasonality parameters were extracted as follows:

iv. Seasonal maximum: highest raw NDVI value in a given growing season.

v. Seasonal NDVI mean: an average of all raw NDVI values between SOS and EOS.

The smoothing methodology applied to the NDVI data was also used to derive seasonality metrics from the 16 day rainfall time series. For each wet season, the total wet season rainfall was calculated as the sum of all raw 16 day values that fell between the respective rainfall SOS and EOS. Finally, each rainfall seasonality or LSP metric consisted of a series of 12 data points, one from each season over the 2001–2012 period.

2.5 Rainfall–NDVI correlations

First, we used time-series analysis to study the strength of the association between the 16 day rainfall and NDVI time series. The cross-correlation function measures the similarity between two time series as a function of a time-lag applied to one of them. In this case, it outputs Pearson's correlations between the rainfall and NDVI time series for lags 0 to n (where n is the maximal lag in days) applied to the rainfall series. The

BGD
12, 981–1013, 2015

cross-correlation function is defined as:

$$r_n = \frac{\mathrm{Cov}_n(\mathrm{rainfall, NDVI})}{\mathrm{SD}_{\mathrm{rainfall}}\mathrm{SD}_{\mathrm{NDVI}}} \quad (2)$$

Where r_n is the cross-correlation coefficient at lag n, Cov is the covariance between the two time series while SD refers to the standard deviation. The cross-correlation analysis was conducted for each site starting with a lag of the NDVI series of 0 (concurrent 16 day window, $n = 0$) up to a lag of 6×16 days (3 months, $n = 6$). The maximum r_n from the resulting pool of lagged coefficients is then taken to represent that site's strongest vegetation response to prior rainfall conditions. To get a finer impression of the spatial variation in the rainfall–NDVI correlation, the cross-correlation analysis was also performed on the NDVI time series of each pixel (i.e., at the 250 m spatial resolution).

In the second part of this analysis, a Pearson's correlation matrix was computed for all the phenological and rainfall seasonality metrics i.e., for each unique pair between a rainfall seasonality metric and an LSP metric, a Pearson's correlation coefficient was calculated.

Finally, to assess the rainfall and NDVI trend over the short-term (2001–2012), each seasonality metric was regressed against year.

A significance threshold of $\alpha = 0.05$ was used for all statistical analyses discussed in this paper.

3 Results

3.1 Long term trends in rainfall

The initial regression of rainfall against time using all available data from 1969 to 2012 (Model I, Fig. 2) yielded a decline of 5.80 mm yr^{-1} in total annual rainfall ($p = 0.06$, adjusted $r^2 = 0.064$, standard error (SE) = ±2.99 mm). Notably, 1998, which coincides with an El-Niño event was extremely wet. It was also the wettest year on Aldabra since 1969. In a second regression model (Model II, Fig. 2), we treated 1998 as an outlier. This analysis yielded a significant decline in total annual rainfall of 6.63 mm yr^{-1} (p = 0.016, adjusted r^2 = 0.12, SE = ±2.64 mm); hence this outlier has little impact on the estimate. To assess the possible impact of the missing rainfall data from October 1976, we interpolated this value using a mean based on all available data. This model gave a slope estimate of −5.80 mm yr^{-1} (p = 0.06, adjusted r^2 = 0.064, SE = ±2.99 mm). Once again, excluding 1998 from this model yielded a slope of −6.64 mm yr^{-1} (p = 0.016, adjusted r^2 = 0.12, SE = ±2.64 mm); hence the estimate is also robust to the inclusion of the 1976 rainfall data.

We further split the annual rainfall into wet season (November–April) and dry season (May–October) totals. For the wet season totals there was a significant decline of −5.74 mm yr^{-1}, (p = 0.01, adjusted r^2 = 0.13, SE = ±2.13 mm; excluding 1998), and for the dry season a non-significant decline of −1.42 mm yr^{-1}, (p = 0.18, adjusted r^2 = 0.02, SE = ±1.05 mm; excluding 1998). Therefore, the decline in annual rainfall appears to be mostly due to reduced wet season rainfall, a trend that coincides with the wider East African region (Funk et al., 2008; Lyon and DeWitt, 2012).

3.2 Dendroecology

Despite the presence of rings (Fig. 3), absence of clear tree-ring wood anatomical structures and of common and consistent ring-width patterns between samples, within and across sampling sites impeded precise cross-dating. Information such as absolute age of the trees or periodicity of cambial activity in the species on Aldabra would have reduced cross-dating uncertainties, e.g., as shown by Nicolini et al. (2010) with *Acacia seyal* from Niger.

Due to the described limitations, we were unable to link the tree-ring chronologies to the long-term rainfall record (1969–2012) or, use the tree-ring data to assess long-term trends in Aldabra's productivity. However, as outlined in the discussion section, this result is still of ecological importance with regard to how woody types on Aldabra respond to seasonal and inter-annual changes in rainfall as compared to tortoise turf.

3.3 Rainfall–NDVI seasonality patterns over 2001–2012

NDVI time series of all six sites followed similar annual cycles (Fig. 4). Based on the mean annual NDVI time series (January–December) averaged from 2001 to 2012 data, NDVI minima ranged from 0.44 (Polymnie) to 0.56 (Malabar) while the maxima ranged from 0.58 (GTSC) to 0.71 (Malabar). Similar to the atoll-wide mean NDVI (Fig. 4), all six sites exhibited distinct unimodal seasonality, consistent with the pattern in the rainfall time series. In addition, there is no discernible upward or downward inter-annual trend in rainfall or in NDVI for 2001–2012.

3.4 Rainfall–NDVI correlations

The strongest rainfall–NDVI correlation occurred at a lag of one to four 16 day periods, depending on the site. This means that an NDVI observation from a given 16 day period is most strongly associated with rainfall from either the previous 16 day window (lag 1) or the 2nd–4th preceding periods (lags 2–4). Picard and Polymnie appear to have shorter lag periods than Grande Terre and Malabar. For all study units on Grande Terre, the maximal rainfall–NDVI correlation occurred at a lag of three 16 day periods, corresponding to an approximate six week time difference between rainfall changes and ensuing vegetation responses (Table 2).

Figure 5 shows the spatial variation in the magnitude of rainfall–NDVI correlations (r_n) at the pixel resolution. Spatial patterns in these correlations that correspond to the distribution of different vegetation types and their sensitivity to water stress can be discerned. GTE, which has the highest percentage cover of tortoise turf, has the highest correlation between rainfall and NDVI, suggesting that tortoise turf are particularly sensitive to changes in rainfall. Areas along the lagoon shores (mangrove

BGD
12, 981–1013, 2015

dominated) have the lowest r_n values with the exception of Malabar which unlike other sites, has low r_n values along the lagoonal shores and in most of its inland regions.

Correlation analysis of rainfall seasonality and NDVI-derived vegetation phenological metrics revealed clear spatial patterns in the strength of the relationship between wet season total rainfall and corresponding growing season NDVI (Table 3). Year 2007 was excluded as an outlier because, compared to other years, its growing season mean and maximum NDVI (atoll-wide) were unusually high for the corresponding wet season rainfall amount, e.g. there is a correlation between maximum growing season NDVI (atoll wide) and wet season rainfall ($r = 0.68$, $p = 0.02$, $n = 11$) only with the exclusion of year 2007 (Fig. A2). Correlation between mean growing season NDVI and total wet season rainfall on the other hand borders on statistical significance ($r = 0.58$, $p = 0.06$) when the 2007 season is excluded.

Unlike other years, the 2007 wet season appears bimodal (Fig. 4). Its second "hump" occurs beyond the respective wet season EOS as designated by the Savitzky–Golay smoother (Fig. 4), possibly resulting in an underestimation of the 2007 wet season rainfall and hence the outlier effect (Fig. A2). This illustrates a typical challenge in parameterization of noisy time series by smoothing, i.e., it is sometimes difficult to optimize the smoother's fit both locally and globally.

Significant Pearson correlation coefficients (between rainfall and NDVI seasonality metrics) are only significant upon exclusion of year 2007 data (Table 3). For brevity, we present and discuss results from four sites, where at least one significant correlation coefficient between an LSP metric and a rainfall seasonality metric was observed. This excludes GTSC and Picard.

We did not find significant temporal trends in any of the rainfall or NDVI seasonality metrics for the 2001–2012 period.

BGD
12, 981–1013, 2015

4 Discussion

4.1 Rainfall–vegetation dynamics and their implications

Aldabra's dry season NDVI minimum is high compared to other areas with similar rainfall regimes e.g., Fuller and Prince reported a dry season NDVI minimum below 0.2 both for "wet" and "dry" vegetation types in Southern Africa (Fuller and Prince, 1996). This concurrence of high dry season NDVI minima with strong seasonality patterns and distinct spatial trends in the strength of rainfall–NDVI correlations is evidence of varied responses to rainfall fluctuations in different vegetation types.

Deciduous vegetation types, e.g., tortoise turf are probably the main contributors to the seasonality observed in the NDVI time series. In contrast, facultative deciduous and evergreen vegetation types such as Pemphis are the most likely source of the high background signal (and therefore high dry season NDVI). These differences can in turn be assigned to differences in plant physiology. Being more deeply rooted, shrub and woody species, e.g., *O. ciliata*, are likely to be less vulnerable to droughts than the shallower rooted species that comprise the tortoise turf. Inter-annual coupling between NDVI and rainfall is particularly strong on GTE and Malabar (Table 3). Strong rainfall–NDVI correlations in Pemphis areas (Table 3) may indicate that Pemphis-dominated vegetation contains considerable amounts of deciduous species. Aldabra's susceptibility to drought is therefore evident across its entire landscape.

As there are clear correlations between rainfall and productivity throughout the season, and clear evidence that rainfall is declining over the long-term, there must be some concern over the long-term future of the tortoise population. The tortoises occur throughout the atoll, but different vegetation types support different densities of animals (Turnbull et al., 2015). The open mixed scrub habitat common on Eastern Grand Terre supports the highest densities of tortoises, and tortoises exhibit strong seasonal movements to exploit this habitat during the wet season. A decline in the productivity of this vegetation type would therefore appear to be particularly detrimental to the population as a whole.

BGD
12, 981–1013, 2015

Detailed monitoring of the tortoise populations on twelve transects around the atoll over the last twenty years reveals that current populations appear to be stable (Turnbull et al., 2015); however, previous work seemed to suggest that there had been an earlier population crash on Eastern Grand Terre that might have been the result of rainfall declines and the subsequent loss of important shade trees (Bourn et al., 1999). The well-being of the tortoise population may therefore depend on multiple vegetation types. As water stress is expected to intensify over East Africa towards 2050 (Parry, 2007), continued monitoring is essential in order to have an early warning signal in the event of drastic or prolonged declines in vegetation performance.

The absence of clear and consistent tree-rings in *O. ciliata* indicates that shrub and woody vegetation are less sensitive to seasonal rainfall fluctuations than the tortoise turf. As such, distinct tree-rings may form only when dry season rainfall is extremely low or infrequent, as in some other semi-arid ecosystems (Cherubini et al., 2003; Battipaglia et al., 2014). Despite the congruence between leaf fall phenology and rainfall seasonality in *O. ciliata*, the tree has been described as an "obligate deciduous" species with "minute" responses to dry season rainfall (Gibson and Phillipson, 1983b). Our tree-ring and wood anatomical observations show that cambial growth might occur intermittently over the dry season, impeding our ability to deduce the periodicity of ring formation in the species by way of cross-dating alone. Given Aldabra's karstic physiography (Stoddart, 1968), access to fresh ground water during the dry season is also plausible.

4.2 The role of rainfall in the context of other factors that limit growth

Dry season stressors on Aldabra are not exclusively limited to water availability. For example, grazing pressure on the tortoise turf intensifies as the dry season progresses (Gibson and Phillipson, 1983a) although this is to some extent ameliorated by the movement of animals away from the coastal areas. Onshore south-east monsoon winds exert tremendous physical force on exposed coastal shrub, resulting in deformation of their growth forms towards the wind direction. However, shrubs in

BGD
12, 981–1013, 2015

general exhibit some degree of tolerance to the harsh south-east monsoons and associated salt sprays. Coastal grasses on the other hand are less resilient to the winds and salt sprays, yet, still have to withstand grazing and water stress in the dry season (Merton et al., 1976). Responses to the same stressors vary even within functional groups, e.g., within the tortoise turf, *Sclerodactylon macrostachyum* tolerates salinity better than the *Sporobolus virginicus*, while the latter can better withstand grazing and trampling by tortoises (Hnatiuk and Merton, 1979). Exact responses and adaptive capacities of different species to water stress in particular is therefore a complex phenomenon that would need on-site studies to comprehend fully. Our research furthers this line of inquiry by highlighting the role of rainfall as the major climatic factor driving productivity cycles on Aldabra Atoll.

In semi-arid tropical ecosystems where rainfall is the main factor limiting growth, soils also play a major role in determining vegetation responses to rainfall. On GTE, the uppermost soil layer in which tortoise turf species are rooted is generally sandy in texture, implying poor water retention capacity (Trudgill, 1979). The strong correlation between the length of the wet season and that of the (NDVI derived) growing season on GTE highlights the importance of extended rainfall periods. Long rainfall seasons allow more time for plants to utilize water resources, thus resulting in longer periods of adequate food supply for the tortoises. Therefore, the sustainability of Aldabra's vegetation in the face of a changing climate relies on future trends in both amount and temporal distribution of wet season rainfall.

4.3 Data limitations

Due to logistical limitations, Aldabra's rainfall has been recorded most reliably and at a daily resolution only at the research station on Picard. Therefore, our analyses of rainfall–NDVI relationships do not account for the spatial variability in rainfall across the atoll noted in earlier studies using monthly rainfall data from multiple locations (Hnatiuk, 1979). However, the excellent agreement of the spatial distribution of Aldabra's vegetation (based on the evergreen vs. deciduous functional distinction)

BGD
12, 981–1013, 2015

with that of LSP responses to rainfall shows that this record is indeed suitable for atoll-wide applications. At the same time, setting up the infrastructure to build similar data records across the atoll would help to better contextualize rainfall–vegetation dynamics and should be considered in the future.

5 Conclusions

Based on the strong coupling between Aldabra's rainfall and NDVI, we conclude that further declines in rainfall are likely to impact the atoll's ecosystem. The nature and extent of these impacts will depend on the severity of these changes and the ability of Aldabra's flora and fauna to adapt. Areas dominated by tortoise turf vegetation, the main food source for many of Aldabra's giant tortoises during the wet season showed the greatest sensitivity to seasonal and inter-annual rainfall fluctuations. Coupled with the observed decline in Aldabra's wet season rainfall, the dependence of terrestrial productivity on rainfall could place the tortoise population in a vulnerable position.

Finally, this study shows that useful ecological information can be obtained through careful wood anatomical observations linked to dendrochronological analyses from tropical shrubs even if an exact identification of tree-ring borders in such species may be hard or impossible. Questions on past productivity trends in tropical islands can potentially be addressed using dendrochronological techniques, but only if the dry season is reliably prolonged or severe.

Acknowledgements. We thank the Seychelles Islands Foundation for the excellent research collaboration within which this study was realized, Aurélie Duhec, Sam Balderson, Naomi Doak and Janske van de Crommenacker for compiling the rainfall datasets, Andy Goufe, Martijn van Dinther and Caterina Onezia for sampling the tree cores, Holger Gärtner (WSL, Birmensdorf) for overseeing the wood anatomy study and we appreciate the technical assistance given to us at the WSL by Loïc Schneider, Anne Verstege and Christian Ginzler. We thank the University of Zurich for the support through the Zurich Aldabra Research Platform (ZARP) and the University Research Priority Programme on Global Change and Biodiversity (URPP GCB).

BGD
12, 981–1013, 2015

NDVI data were freely obtained online through the MODIS global subsetting tool at the Oak Ridge National Laboratory Distributed Active Archive Centre.

References

Battipaglia, G., De Micco, V., Brand, W. A., Saurer, M., Aronne, G., Linke, P., and Cherubini, P.: Drought impact on water use efficiency and intra-annual density fluctuations in Erica arborea on Elba (Italy), Plant Cell Environ., 37, 382–391, doi:10.1111/pce.12160, 2014.

Bourn, D., Gibson, C., Augeri, D., Wilson, C. J., Church, J., and Hay, S. I.: The rise and fall of the Aldabran giant tortoise population, P. Roy. Soc. B-Biol. Sci.. 266, 1091–1100, doi:10.1098/rspb.1999.0748, 1999.

Cherubini, P., Gartner, B. L., Tognetti, R., Bräker, O. U., Schoch, W., and Innes, J. L.: Identification, measurement and interpretation of tree rings in woody species from mediterranean climates, Biol. Rev. Camb. Philos., 78, 119–148, doi:10.1017/S1464793102006000, 2003.

Dai, A., Trenberth, K. E., and Qian, T.: A global dataset of Palmer drought severity index for 1870–2002: relationship with soil moisture and effects of surface warming, J. Hydrometeorol., 5, 1117–1130, doi:10.1175/JHM-386.1, 2004.

Easterling, D. R.: Climate extremes: observations, modeling, and impacts, Science, 289, 2068–2074, doi:10.1126/science.289.5487.2068, 2000.

Eklundh, L.: Vegetation index trends for the African Sahel 1982–1999, Geophys. Res. Lett., 30, 1430, doi:10.1029/2002GL016772, 2003.

Farrow, G. E.: The climate of Aldabra Atoll, Philos. T. Roy. Soc. B, 260, 67–91, doi:10.1098/rstb.1971.0007, 1971.

Fichtler, E., Trouet, V., Beeckman, H., Coppin, P., and Worbes, M.: Climatic signals in tree rings of *Burkea africana* and *Pterocarpus angolensis* from semiarid forests in Namibia, Trees, 18, 442–451, doi:10.1007/s00468-004-0324-0, 2004.

Fuller, D. and Prince, S.: Rainfall and foliar dynamics in tropical southern Africa: potential impacts of global climatic change on savanna vegetation, Climatic Change, 33, 69–96, 1996.

Funk, C., Dettinger, M. D., Michaelsen, J. C., Verdin, J. P., Brown, M. E., Barlow, M., and Hoell, A.: Warming of the Indian Ocean threatens eastern and southern African food security but could be mitigated by agricultural development, P. Natl. Acad. Sci. USA, 105, 11081–11086, doi:10.1073/pnas.0708196105, 2008.

BGD
12, 981–1013, 2015

Garonna, I., de Jong, R., de Wit, A. J. W., Mücher, C. A., Schmid, B., and Schaepman, M. E.: Strong contribution of autumn phenology to changes in satellite-derived growing season length estimates across Europe (1982–2011), Glob. Change Biol., 20, 1–14, doi:10.1111/gcb.12625, 2014.

Gibson, C. W. D. and Phillipson, J.: The primary production of Aldabra atoll, with reference to habitats used by giant tortoises, Philos. T. Roy. Soc. B, 302, 167–199, doi:10.1098/rstb.1983.0050, 1983a.

Gibson, C. W. D. and Phillipson, J.: The vegetation of Aldabra Atoll: preliminary analysis and explanation of the vegetation map, Philos. T. Roy. Soc. B, 302, 201–235, doi:10.1098/rstb.1983.0051, 1983b.

Hansen, D. M., Donlan, C. J., Griffiths, C. J., and Campbell, K. J.: Ecological history and latent conservation potential: large and giant tortoises as a model for taxon substitutions, Ecography, 33, 272–284, doi:10.1111/j.1600-0587.2010.06305.x, 2010.

Hnatiuk, R. J.: Temporal and spatial variations in precipitation on Aldabra, Philos. T. Roy. Soc. B, 286, 25–33, doi:10.1098/rstb.1979.0013, 1979.

Hnatiuk, R. and Merton, L.: A perspective of the vegetation of Aldabra, Philos. T. Roy. Soc. B, 286, 79–84, 1979.

Holben, B. N.: Characteristics of maximum-value composite images from temporal AVHRR data, Int. J. Remote Sens., 7, 1417–1434, doi:10.1080/01431168608948945, 1986.

Huete, A., Didan, K., Miura, T., Rodriguez, E. P., Gao, X., and Ferreira, L. G.: Overview of the radiometric and biophysical performance of the MODIS vegetation indices, Remote Sens. Environ., 83, 195–213, doi:10.1016/S0034-4257(02)00096-2, 2002.

Jönsson, P. and Eklundh, L.: TIMESAT – a program for analyzing time-series of satellite sensor data, Comput. Geosci.-UK, 30, 833–845, doi:10.1016/j.cageo.2004.05.006, 2004.

Lyon, B. and DeWitt, D. G.: A recent and abrupt decline in the East African long rains, Geophys. Res. Lett., 39, L02702, doi:10.1029/2011GL050337, 2012.

Merton, L., Bourn, D., and Hnatiuk, R.: Giant tortoise and vegetation interactions on aldabra atoll – Part 1: Inland, Biol. Conserv., 9, 293–304, doi:10.1016/0006-3207(76)90051-3, 1976.

Metcalfe, A. V. and Cowpertwait, P. S. P.: Introductory Time Series with R, Springer New York, New York, NY, 2009.

Mimura, N., Nurse, L., McLean, R. F., Agard, J., Briguglio, L., Lefale, P., Payet, R., and Sem, G.: Small islands, in: Climate Change 2007: Impacts, Adaptation and Vulnerability. Contribution of Working Group II to the Fourth Assessment Report of the Intergovernmental Panel on

BGD
12, 981–1013, 2015

Primary productivity and its correlation with rainfall on Aldabra Atoll

J. Shekeine et al.

Climate Change, edited by: Parry, M. L., Canziani, O. F., Palutikof, J. P., van der Linden, P. J., and Hanson, C. E., Cambridge University Press, Cambridge, UK, 687–716, 2007.
Mu, Q., Zhao, M., Kimball, J. S., McDowell, N. G., and Running, S. W.: A remotely sensed global terrestrial drought severity index, B. Am. Meteorol. Soc., 94, 83–98, doi:10.1175/BAMS-D-11-00213.1, 2013.
Nicolini, G., Tarchiani, V., Saurer, M., and Cherubini, P.: Wood-growth zones in Acacia seyal Delile in the Keita Valley, Niger: is there any climatic signal?, J. Arid Environ., 74, 355–359, doi:10.1016/j.jaridenv.2009.08.017, 2010.
Oak Ridge National Laboratory Distributed Active Archive Center (ORNL DAAC): MODIS subsetted land products, Collect. 5, available at: http://daac.ornl.gov/MODIS/modis.html (last access: 1 June 2013), 2011.
Omuto, C. T., Vargas, R. R., Alim, M. S., and Paron, P.: Mixed-effects modelling of time series NDVI-rainfall relationship for detecting human-induced loss of vegetation cover in drylands, J. Arid Environ., 74, 1552–1563, doi:10.1016/j.jaridenv.2010.04.001, 2010.
Osipova, E., Shi, Y., Kormos, C., Shadie, P., C., Z., and Badman, T.: IUCN World Heritage Outlook 2014: a Conservation Assessment of All Natural World Heritage Sites, IUCN, Gland, Switzerland, 2014.
Parry, M.: Climate Change 2007: Impacts, Adaptation and Vulnerability: Working Group II Contribution to the Fourth Assessment Report of the IPCC Intergovernmental Panel on Climate Change, Cambridge University Press, Cambridge, United Kingdom, 2007.
Potter, C., Klooster, S., and Genovese, V.: Net primary production of terrestrial ecosystems from 2000 to 2009, Climatic Change, 115, 365–378, doi:10.1007/s10584-012-0460-2, 2012.
Regent Instruments Inc.: WinDendro Reference Manual, Version 2008a, Régent Instruments Québec, Québec, 2008.
Rossi, L., Sebastiani, L., Tognetti, R., D'Andria, R., Morelli, G., and Cherubini, P.: Tree-ring wood anatomy and stable isotopes show structural and functional adjustments in olive trees under different water availability, Plant Soil, 372, 567–579, doi:10.1007/s11104-013-1759-0, 2013.
Schweingruber, F. H.: Tree rings-basics and applications of dendrochronology., 1st Edn., Kluwer Academic Publishers, Dordrecht, Holland, 1988.
Stoddart, D.: The conservation of Aldabra, Geogr. J., 134, 471–485, 1968.
Stoddart, D. R. and Mole, L. U.: Climate of Aldabra Atoll Research Bulletin, 202, 1–21, doi:10.5479/si.00775630.202.1, 1977.

BGD
12, 981–1013, 2015

Stokes, M. and Smiley, T.: An Introduction to Tree-Ring Dating, 1st Edn., University of Chicago Press, Chicago, USA, 1968.
Trudgill, S. T.: The soils of Aldabra, Philos. T. Roy. Soc. B, 286, 67–77, doi:10.1098/rstb.1979.0016, 1979.
Turnbull, L. A., Arpat, O., Wilna, A., Rich, B., Lindsay, C., Jock, C., Naomi, D., Hansen, D. M., Pistorius, P., Richards, H., van de Crommenacker, J., von Brandis, R., Frauke, F.-D., and Bunbury, N.: Sympatric subpopulations of endemic Aldabra giant tortoises have distinctive stable morphotypes, P. Roy. Soc., submitted, 2015.
Whittaker, R. J. and Fernández-Palacios, J. M.: Island biogeography: ecology, evolution, and conservation, Oxford University Press, Wiltshire, UK, 2007.
Zhao, M. and Running, S. W.: Drought-induced reduction in global terrestrial net primary production from 2000 through 2009, Science, 329, 940–943, doi:10.1126/science.1192666, 2010.

BGD
12, 981–1013, 2015

Table 1. Summary of NDVI (normalized difference vegetation index) time series for the six study sites. RMSE (Root Mean Squared Error) values represent the deviation of the respective site's smoothed NDVI time series (from which phenological parameters were derived) relative to that site's raw NDVI time series.

Site	Area (km^2)	Number of pixels	RMSE
Grande Terre East	66.7	1067	0.00048
Grande Terre South West	36.8	590	0.00124
Malabar	30.5	488	0.00274
Grande Terre South-Central	16.4	263	0.00189
Picard	7	113	0.00542
Polymnie	2	32	0.00819
Total	159.4	2553	

BGD
12, 981–1013, 2015

Table 2. Maximal cross-correlations (r_n) between NDVI (normalized difference vegetation index) and rainfall time series and the respective time lags (in months).

NDVI series	r_n	Lag
Grande Terre East	0.49	1.6
Grande Terre South-Central	0.43	1.6
Grande Terre South West	0.50	1.6
Malabar	0.36	2.1
Picard	0.29	1.1
Polymnie	0.28	0.5

BGD
12, 981–1013, 2015

Table 3. Pearson correlations between NDVI (normalized difference vegetation index) and rainfall seasonality metrics for four study sites. Coefficients marked with an asterisk (*) are statistically significant at the 95 % confidence level.

	Total wet season rainfall	Wet season length
Grande Terre East		
Growing season maximum NDVI	0.39	0.17
Growing season mean NDVI	0.65*, $p = 0.03$	−0.10
LOS (NDVI)	0.09	0.74*, $p = 0.01$
Grande Terre South-West		
Growing season maximum NDVI	0.73*, $p = 0.01$	0.13
Growing season mean NDVI	0.46	−0.15
Length of season (NDVI)	0.29	0.59
Malabar		
Growing season maximum NDVI	0.64*, $p = 0.04$	−0.01
Growing season mean NDVI	0.64*, $p = 0.04$	−0.11
Length of season (NDVI)	0.31	0.55
Polymnie		
Growing season maximum NDVI	−0.01	−0.02
Growing season mean NDVI	0.72*, $p = 0.01$	0.21
Length of season (NDVI)	−0.25	−0.12

BGD
12, 981–1013, 2015

Table B1. Total monthly rainfall (in millimetres) on Aldabra based on rain-gauge readings at Picard station. Source: Seychelles Islands Foundation.

Year	Jan	Feb	Mar	Apr	May	Jun	Jul	Aug	Sep	Oct	Nov	Dec
1969	153.4	147.2	151.5	393.5	176.3	36.8	39.7	14.3	18.5	11.8	54.9	56.8
1970	47.5	85.2	139.6	210.5	31.7	29.5	33.7	25.7	7.3	20.9	12.7	56.6
1971	244.5	57.4	246.6	192.5	34.7	65.9	14.3	19.1	8.6	6	88.7	200.4
1972	224.5	15	112.2	162.2	28.2	100.3	54.6	75.1	4.2	12.7	25.6	240.2
1973	261	286.8	262.8	56.7	57.1	47.7	81.3	25.2	21.8	33.7	9.2	77.6
1974	290.6	114.5	380.8	346.4	50.4	29.4	51.2	31.8	1.9	1.1	19.4	148.9
1975	131.4	162.8	111.1	166.7	76.7	41.4	16.1	14.9	14.5	2.9	91.7	136.2
1976	357.4	177.4	260.9	87.1	66.6	64.4	65.5	36	4.7	NA	16.7	79.8
1977	262.5	116.3	255.7	239.4	139.6	89.5	82.2	26.8	5	37	63.5	120.8
1978	254	139.2	339	18	54.8	48.1	135.4	22.6	8.7	16.9	191.6	234.4
1979	233.6	108.6	105.2	67.8	140.3	55.3	61.4	33.7	19.4	0.1	52.3	262.2
1980	82.1	151.9	120.8	184.9	19.1	66.1	16.6	40	10	1.6	9.5	123.1
1981	143.5	52.9	238.1	17.8	94.5	26.2	22.1	20.4	12.1	8.6	10.8	337.1
1982	91.4	44.8	121.2	136.8	70.1	106.9	12.9	17.2	40.9	47.5	110.4	34.6
1983	481.4	108.8	140.2	51.4	146	12.4	12	24.6	5.5	30.7	65.3	228.9
1984	81.5	56	137.5	74.4	19.3	48.5	15.1	2.8	1	6.6	27.1	117.3
1985	58.4	212.4	162.3	116.6	24.9	46.9	24.9	18.5	2.8	10.9	38.4	168.3
1986	263.7	10.6	128.4	116.3	118.5	44.2	56.2	11.7	5.7	4.7	92.4	243
1987	78.2	190.5	90.8	126.7	14	23.6	54	48.9	7.6	2.2	125	174.1
1988	195.5	159.6	132.4	15.6	46.7	33.6	22.8	28.5	3.2	5.8	87.6	305.5
1989	85.5	7.2	265	195.9	83.6	32.4	19.3	9.3	5.7	7.8	28.5	194.5
1990	264.2	83.2	35	197.8	28.5	5.7	15.5	6.7	12.7	6.5	99.1	186.7
1991	336.1	50.7	13.8	47.7	33.6	23.2	12.3	13.1	13.1	7.5	38.5	NA
1992	NA	NA	NA	NA	NA	NA	NA	NA	NA	NA	NA	NA
1993	NA	NA	NA	400	132.2	23	5	25	4	0	7	28
1994	84.4	112	183	63.3	107.8	24.8	14.9	14.5	4.7	235.4	5.3	442.3
1995	53	76.6	306.7	122.4	38.1	18.3	19.6	10.4	10.8	10.4	2	19
1996	145	175.6	301.6	19.7	19.9	36.8	46.5	6.6	3.6	12.4	10.1	70
1997	298.2	0	220.3	48	21.4	19.4	12	9.2	0.8	12.6	227.8	299
1998	332.5	282.6	124.3	246.6	41.2	58.3	37.4	32.6	12.6	8.1	10.2	85.1
1999	246.9	153.7	187.8	4.9	24.9	27.71	28.65	2.9	9.1	4.8	15.7	131.6
2000	50.6	13.4	122	34.4	20	68.4	20.4	21.1	1.7	0.4	22.8	116.3
2001	142.3	229.9	102.3	63.1	42.8	27.3	16.3	41	3.6	80.5	12	102.4
2002	114.2	66	174.8	38.9	9.5	2.7	1.2	2.6	7.4	2.2	35.2	127.5
2003	121.7	44.1	133.9	274	74.4	37.2	31.8	25.7	15.8	4.2	28.5	315
2004	69.5	145.1	11.2	9.1	14.6	7.4	42.9	19	6.2	137	21.5	152.2
2005	249.3	151.85	150.95	170.6	179.45	9.33	38.28	17.58	4.1	5	25.55	77.8
2006	383.3	226	431.4	29.6	43.8	59.2	105.7	83.97	70.91	1.5	87.8	264.9
2007	124.48	22.97	69.11	7.53	17.81	127.8	23.8	16.23	44	5.4	113.8	49
2008	245	51.6	115.9	120.78	6.9	12.6	16.4	5.4	10.7	4.4	76.2	121.7
2009	92	45.9	157.1	91.25	95.5	16	49.6	14.9	5.62	0	10.2	157.55
2010	43.7	243.9	82.66	103.7	70.52	45.24	26.67	20.65	9.65	11.96	6.03	68.31
2011	151.29	149.85	156.31	235.21	85.3	29.38	13.84	21.08	15.7	27.11	96.7	117.65
2012	41.6	262.9	133.6	182	55.7	58.3	27.6	10.3	7.7	2.1	38	183.6

BGD
12, 981–1013, 2015

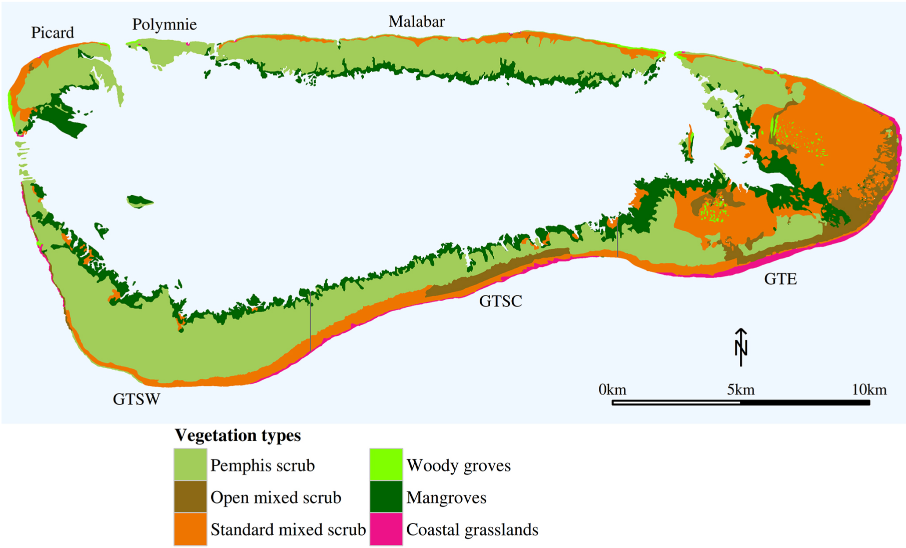

Figure 1. Spatial distribution of vegetation types on Aldabra Atoll based on a 1983 vegetation survey (Gibson and Phillipson, 1983b). This reproduction was prepared by vectorizing the original hard copy. In this study, the southern island of Grande Terre is further split into south-western (GTSW), south-central (GTSC) and eastern (GTE) sub-regions.

BGD
12, 981–1013, 2015

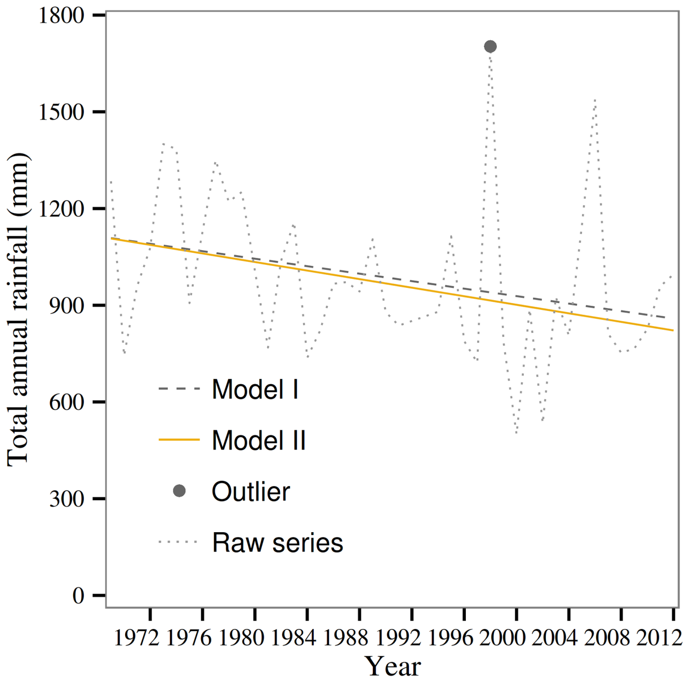

Figure 2. Long term trends in Aldabra's total annual rainfall from rain gauge readings at the Picard research station over the period 1969–2012. An ordinary least squares regression model was used to model total annual rainfall as a function of time (year) (Model I). The model was then refitted with the wettest year on Aldabra's instrumental rainfall record, i.e., 1998, excluded as an outlier thus yielding Model II.

BGD
12, 981–1013, 2015

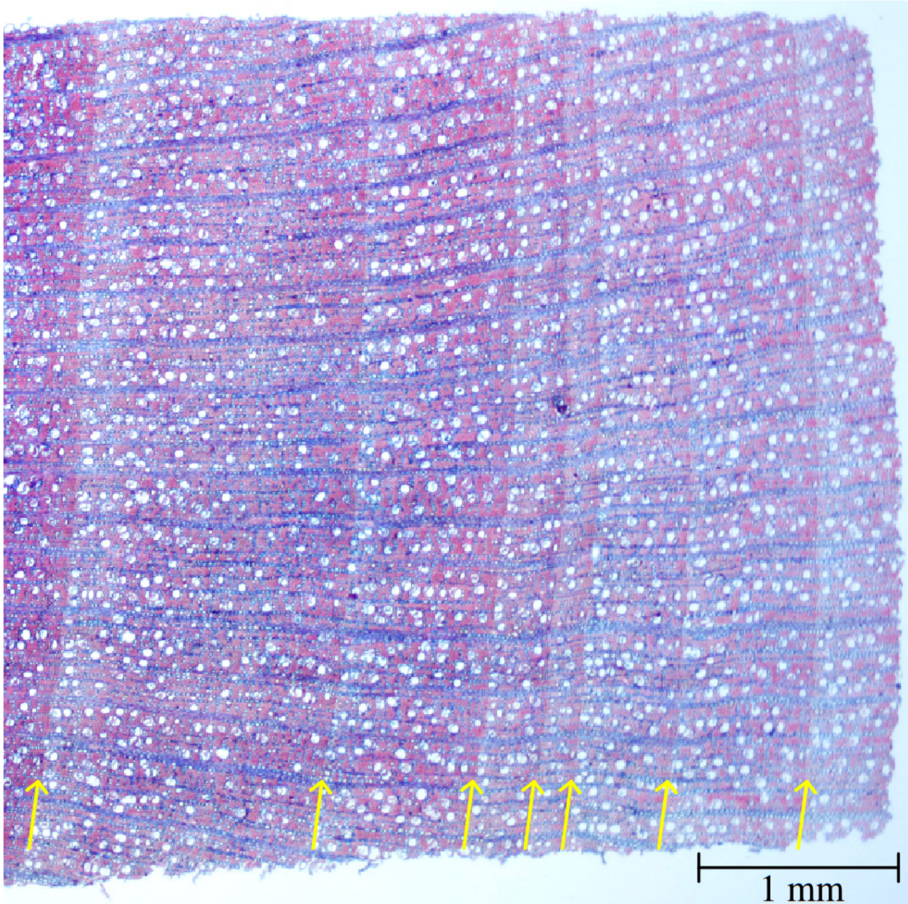

Figure 3. Radial micro-section of an *Ochna ciliata* sample obtained from Picard. Yellow arrows indicate the seven outermost ring boundaries i.e., the image's left to right direction corresponds to the micro-section's pith to bark orientation.

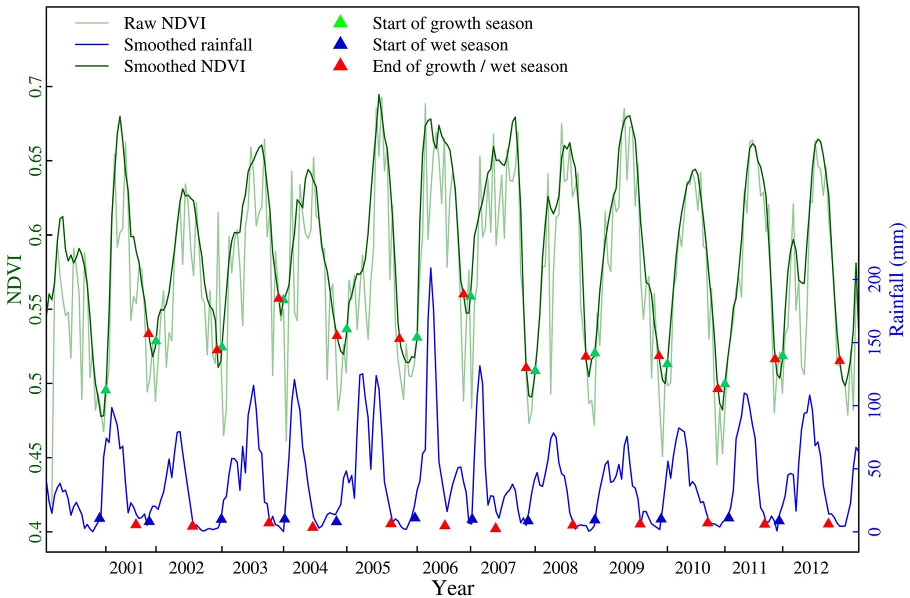

Figure 4. Savitzky–Golay smoothing of Aldabra's rainfall and NDVI (normalized difference vegetation index) time series for the extraction of rainfall and vegetation seasonality parameters. The mean atoll-wide NDVI series is used here to illustrate how the procedure was conducted for each site. Yearly demarcations on the *x* axis are based on the phenological year as defined by the start and end of season points.

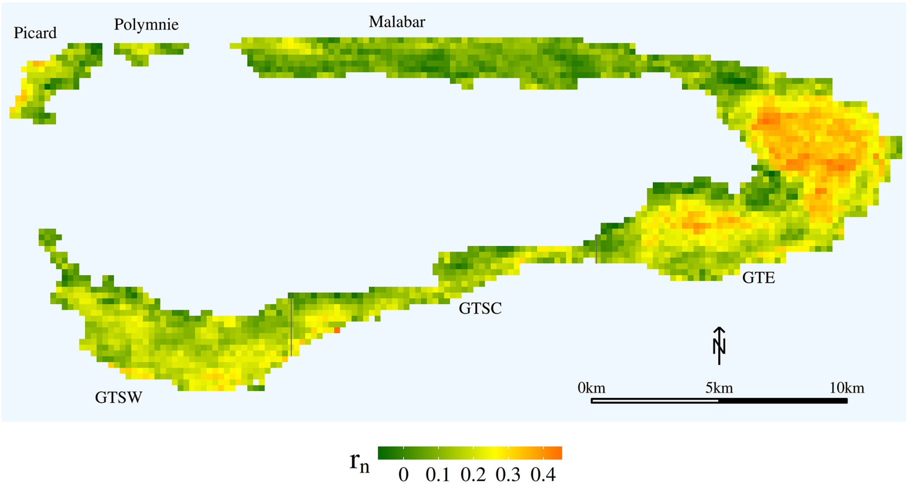

Figure 5. Spatial variation in the strength of rainfall–NDVI cross-correlation (r_n). Coefficients above 0.115 are significant (Fig. A1). Notably, the relationship between NDVI and rainfall is strongest in areas dominated by deciduous types i.e. on GTE. (See Fig. 1 legend for full site names.)

BGD
12, 981–1013, 2015

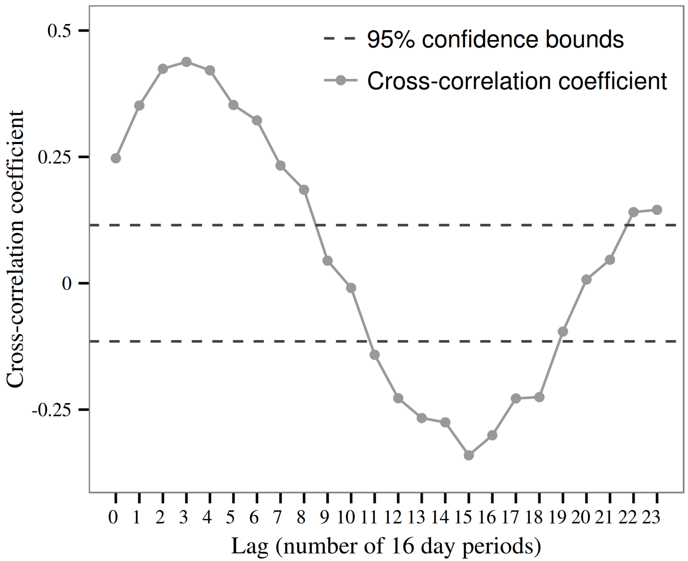

Figure A1. Cross-correlation analysis showing lagged correlation coefficients between rainfall and NDVI (normalized difference vegetation index) time series for up to 23 sixteen day lags (one calendar year). Under the null hypothesis that there is zero correlation between the two time series, the 95 % confidence intervals are $0 \pm 2/\sqrt{N}$ where N is the length of the time series (Metcalfe and Cowpertwait, 2009). NDVI time series of all pixels had a length of 299 (23 values per year covering 13 years). Confidence bounds therefore correspond to cross correlation coefficient values of ±0.115.

BGD
12, 981–1013, 2015

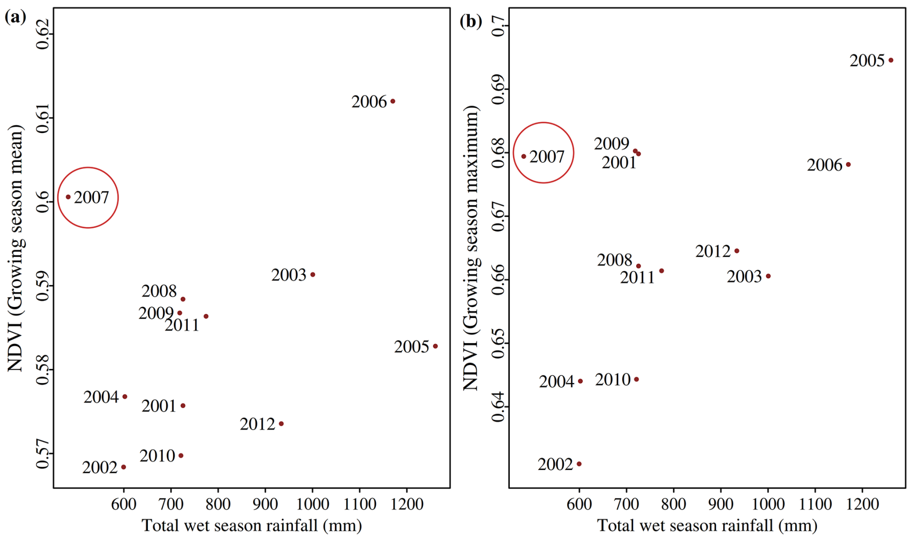

Figure A2. Year 2007's outlier effect in the correlation between wet season rainfall and **(a)** atoll-wide growing season mean NDVI (normalized difference vegetation index); **(b)** atoll-wide growing season maximum NDVI.

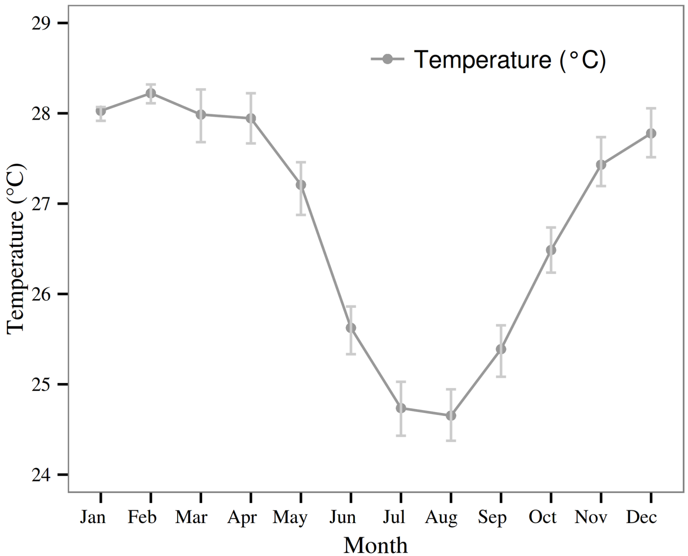

Figure B1. Mean monthly dry-bulb temperatures (± standard error) on Aldabra based on the 1968–2008 average and excluding 1992–1999 for which there is no data. Source: Seychelles Islands Foundation.

BGD
12, 981–1013, 2015